

Supporting Information

All-in-One aPAN/MXene@Ag-Ag₂S Nanofibrous Aerogel for Efficient Oil/Water separation, Solar Interfacial Evaporation and Photocatalytic Degradation of High-concentration Dyes

Busaremu Wulayimujiang [#], Fang Guo [#], Qianyu Ma, Yong Wen, Yang Yang,
Hongyan Huang, Quanpei Xie, Meng Shen, Jinxin Liu^{*}, Si Cheng^{*}

National Engineering Laboratory for Modern Silk, College of Textile and Clothing
Engineering, Soochow University, Suzhou 215123, P. R. China.

E-mail addresses: chengsi@suda.edu.cn (S. Cheng), jxliu@suda.edu.cn (J. Liu).

This supporting information contains the following contents:

Fig. S1. (a) Digital photo of Mxene@Ag-Ag₂S aerogel. (b) Digital photo and mechanical properties of aPAN/MXene@Ag-Ag₂S aerogel.

Fig. S2. (a) SEM of pristine multi-layer Ti₃C₂T_x. (b) Digital photographs of MXene@Ag-Ag₂S colloidal solution with different concentrations (10 mg/mL and 0.01 mg/mL). (c) EDS element analysis of MXene@Ag-Ag₂S. (d) UV-vis-NIR absorption spectra of different aqueous solutions (10 mg/mL).

Fig. S3. XPS spectra of MXene@Ag-Ag₂S.

Fig. S4. (a) The UV-vis absorption spectra of aPAN/MXene@Ag-Ag₂S aerogels for absorption of MB solutions with the concentration of 10 mg/L under dark condition. (b-c) The UV-vis absorption curve of 10 mg/L MB solution of aPAN/MXene (b) and aPAN/MXene@Ag (c), respectively.

Fig. S5. (a) The UV-vis absorption spectra of aPAN/MXene@Ag-Ag₂S aerogels for photocatalytic degradation of MB solutions with the concentration of 100 mg/L. (b) Photodegradation of MB (100 mg/L) for eight cycles using aPAN/MXene@Ag-Ag₂S aerogel. (c, d) The UV-vis absorption curve of aPAN/MXene aerogel of RhB and R6G (10 mg/L), respective.

Fig. S6. (a, b) Solar optical power density curve during photodegradation of dyed oil/water emulsion and dyeing effluents, respectively. (c) UV-vis spectra and corresponding photos of the feed river before and after filtration.

Table S1. The comparison of photodegradation rate towards the MB pollutants of catalysts with those of the counterparts reported in the literatures.

Table S2. Content characteristics of COD and NH₃-N in wastewater before and after degradation.

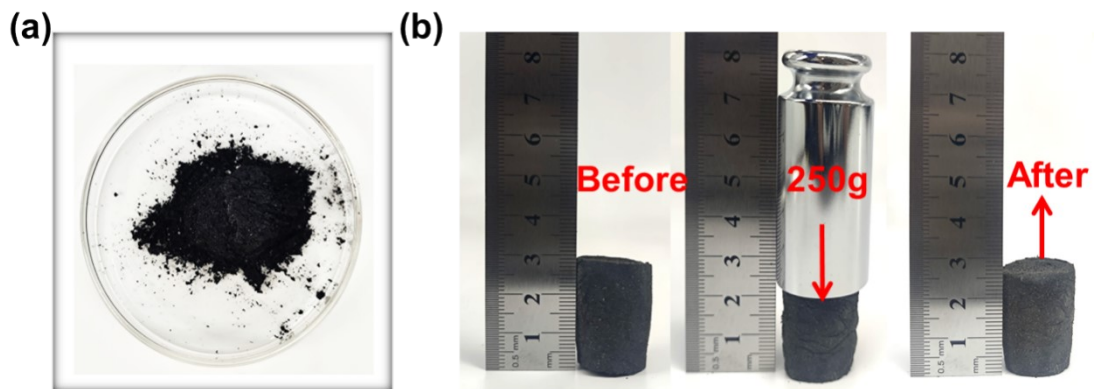


Fig. S1. (a) Digital photo of Mxene@Ag-Ag₂S aerogel. (b) Digital photo and mechanical properties of aPAN/MXene@Ag-Ag₂S aerogel.

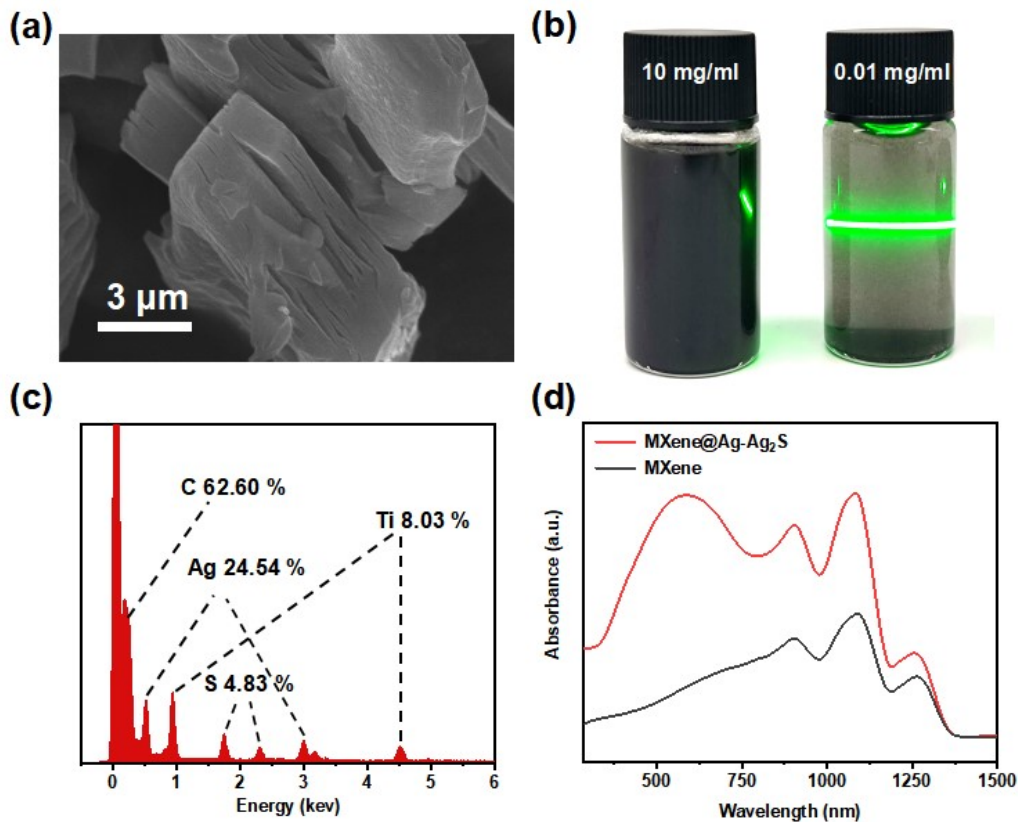


Fig. S2. (a) SEM of pristine multi-layer $\text{Ti}_3\text{C}_2\text{T}_x$. (b) Digital photographs of MXene@Ag-Ag₂S colloidal solution with different concentrations (10 mg/mL and 0.01 mg/mL). (c) EDS element analysis of MXene@Ag-Ag₂S. (d) UV-vis-NIR absorption spectra of different aqueous solutions (10 mg/mL).

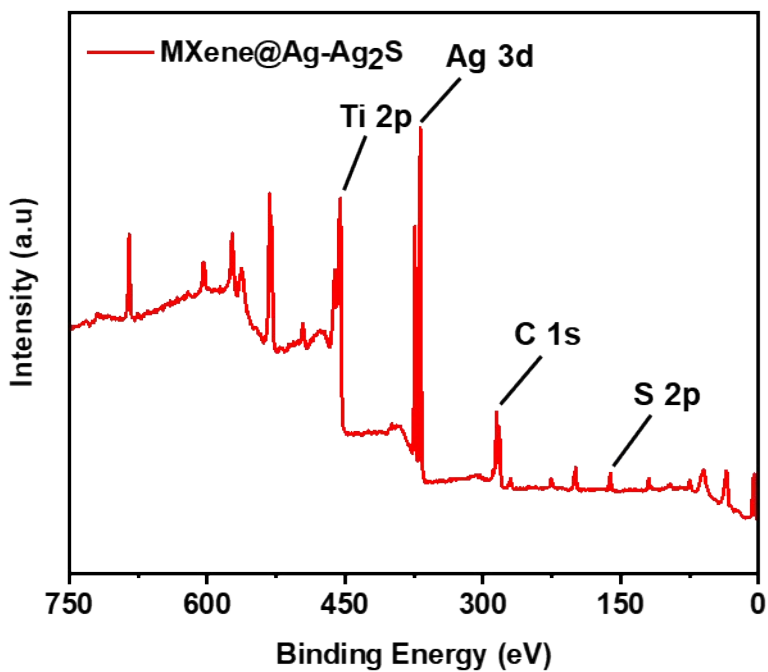


Fig. S3. XPS spectra of MXene@Ag-Ag₂S.

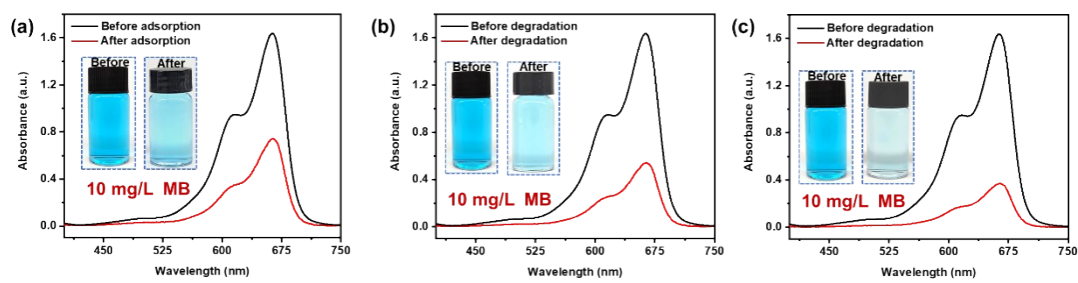


Fig. S4. (a) The UV-vis absorption spectra of aPAN/MXene@Ag-Ag₂S aerogels for absorption of MB solutions with the concentration of 10 mg/L under dark condition. (b-c) The UV-vis absorption curve of 10 mg/L MB solution of aPAN/MXene (b) and aPAN/MXene@Ag (c), respectively.

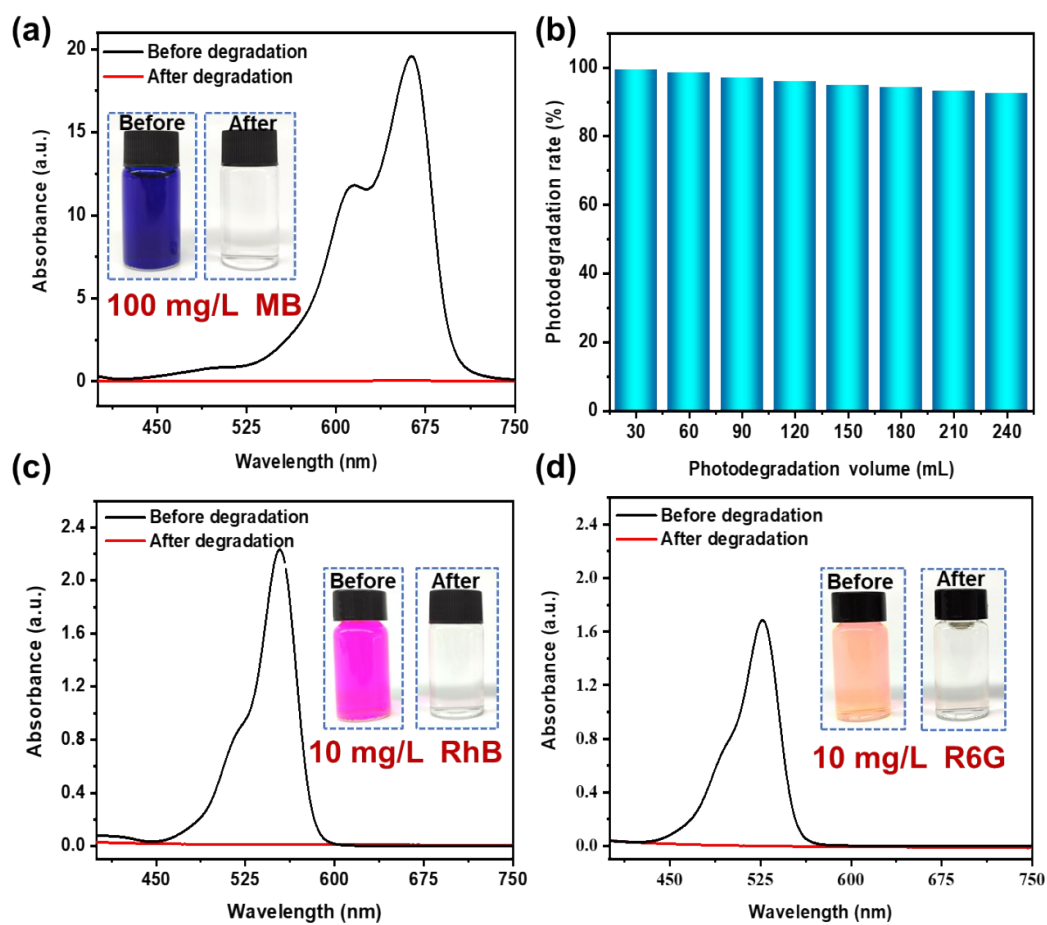


Fig. S5. (a) The UV-vis absorption spectra of aPAN/MXene@Ag-Ag₂S aerogels for photocatalytic degradation of MB solutions with the concentration of 100 mg/L. (b) Photodegradation of MB (100 mg/L) for eight cycles using aPAN/MXene@Ag-Ag₂S aerogel. (c, d) The UV-vis absorption curve of aPAN/MXene aerogel of RhB and R6G (10 mg/L), respective.

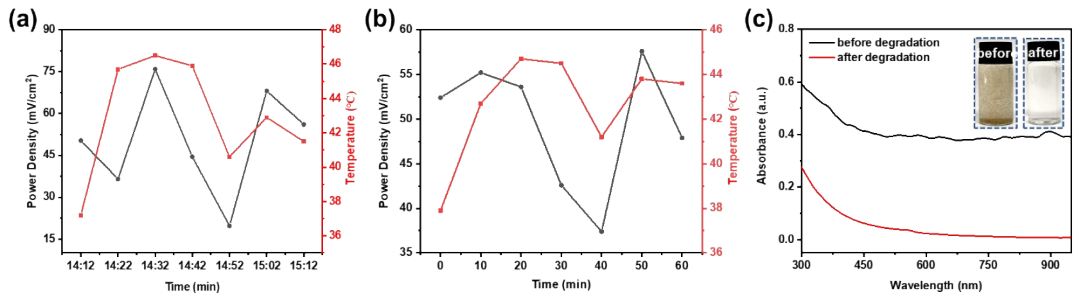


Fig. S6. (a, b) Solar optical power density curve during photodegradation of dyed oil/water emulsion and dyeing effluents, respectively. (c) UV-vis spectra and corresponding photos of the feed river before and after filtration.

Table S1. The comparison of photodegradation rate towards the MB pollutants of catalysts with those of the counterparts reported in the literature.

Materials	Decomposed dye	Dye concentration (mg/L)	Process scale (ml)	Degradation rate (%)	Ref.
aPAN/MXene@Ag-Ag ₂ S	MB	100	240	99.99	This work
Ti ₃ C ₂ Tx/Vit.C(TMAOH)	MB	25	1	100	Ref. ¹
MF-MXene/ppy	MB	10	70	92.38	Ref. ²
MXene@TiO ₂ /PEN	MB	20	50	92.31	Ref. ³
KH570/TiO ₂ /MXene/PAN	MB	20	50	90	Ref. ⁴
ML-Ti ₃ C ₂ (OH) ₂	MB	10	100	81.2	Ref. ⁵
TiO ₂ /MXene	MB	20	60	96.44	Ref. ⁶
Bi ₂ WO ₆ /Nb ₂ CTx	MB	15	100	92.7	Ref. ⁷
Ti ₃ C ₂ MXene/NH ₂ -MIL-88B(Fe)	MB	50	100	~80	Ref. ⁸
Ti ₃ C ₂ Tx	MB	20	100	>90	Ref. ⁹
ZnO@Ti ₃ C ₂	MB	20	20	94.84	Ref. ¹⁰
C/TiO ₂ @TiOF ₂	MB	20	100	95	Ref. ¹¹
AgNPs/TiO ₂ /Ti ₃ C ₂ Tx	MB	10	100	99	Ref. ¹²
ZnO/V ₂ C MXene	MB	10	7.998	98.9	Ref. ¹³
CdS@Ti ₃ C ₂ @TiO ₂	MB	20	200	100	Ref. ¹⁴
Ti ₃ C ₂ /Bi ₂ O ₃	MB/BA	6	500	80	Ref. ¹⁵

Table S2. Content characteristics of COD and NH₃-N in wastewater before and after degradation.

Qing Ke wastewater S2023101815-W001 (DB32/4440-2022)

Main components in wastewater	Discharge Standard	Before degradation	After degradation
COD (mg/L)	30	3.28×10^3	14
NH ₃ -N (mg/L)	1.5	16.2	0.565

References

- 1 D. Bury, M. Jakubczak, M. A. K. Purbayanto, A. Wojciechowska, D. Moszczyńska and A. M. Jastrzębska, *Small Methods*, 2023, 2201252.
- 2 X. Mu, L. Chen, N. Qu, J. Yu, X. Jiang, C. Xiao, X. Luo and Q. Hasi, *J Colloid Interf Sci*, 2023, **636**, 291–304.
- 3 Q. Feng, Y. Zhan, W. Yang, A. Sun, H. Dong, Y.-H. Chiao, Y. Liu, X. Chen and Y. Chen, *J Colloid Interf Sci*, 2022, **612**, 156–170.
- 4 X. Qin, X. Feng, T. Zhu, L. Ji and A. Zhu, *J Solid State Chem*, 2022, **312**, 123142.
- 5 J. Qu, D. Teng, X. Zhang, Q. Yang, P. Li and Y. Cao, *Ceram Int*, 2022, **48**, 14451–14459.
- 6 X. Geng, Y. Liu, W. Xu, X. Huang, P. Wang, M. Zhang, G. Wen and W. Wang, *Ceramics International*, 2022, **48**, 20146–20157.
- 7 C. Cui, R. Guo, H. Xiao, E. Ren, Q. Song, C. Xiang, X. Lai, J. Lan and S. Jiang, *Appl Surf Sci*, 2020, **505**, 144595.
- 8 R. Long, Z. Yu, Q. Tan, X. Feng, X. Zhu, X. Li and P. Wang, *Appl Surf Sci*, 2021, **570**, 151244.
- 9 O. Mashtalir, K. M. Cook, V. N. Mochalin, M. Crowe, M. W. Barsoum and Y. Gogotsi, *J. Mater. Chem. A*, 2014, **2**, 14334–14338.
- 10 M. Liu, J. Li, R. Bian, X. Wang, Y. Ji, X. Zhang, J. Tian, F. Shi and H. Cui, *J Alloy Compd*, 2022, **905**, 164025.
- 11 T. Liu, L. Li, X. Geng, C. Yang, X. Zhang, X. Lin, P. Lv, Y. Mu and S. Huang, *Journal of Alloys and Compounds*, 2022, **919**, 165629.
- 12 Z. Othman, A. Sinopoli, H. R. Mackey and K. A. Mahmoud, *Acs Omega*, 2021, **6**, 33325–33338.

- 13 W. Zhou, B. Yu, J. Zhu, K. Li and S. Tian, *New J Chem*, 2022, **46**, 14793–14804.
- 14 Q. Liu, X. Tan, S. Wang, F. Ma, H. Znad, Z. Shen, L. Liu and S. Liu, *Environ Sci-nano*, 2019, **6**, 3158–3169.
- 15 S. Munir, M. M. Baig, S. Zulfiqar, M. S. Saif, P. O. Agboola, M. F. Warsi and I. Shakir, *Ceram Int*, 2022, **48**, 21676–21689.